Nuclear structure of ^{208}Pb from ^{207}Pb + n resonances

R. Köhler, J. A. Wartena, and H. Weigmann
Commission of the European Communities, Joint Research Center, Geel Establishment, Central Bureau for Nuclear Measurements, Geel, Belgium

L. Mewissen and F. Poortmans
Studiecentrum voor Kernenergie/Centre d'Etude de l'Energie Nucléaire, Mol, Belgium

J. P. Theobald
Institut für Kernphysik, Technische Hochschule, Darmstadt, Federal Republic of Germany

S. Raman
Oak Ridge National Laboratory, Oak Ridge, Tennessee 37831
(Received 27 January 1987)

Resonance structure in the ^{207}Pb + n system has been investigated by measuring the neutron total cross section with high energy resolution and the partial radiative cross sections for transitions to the ground-state and the first-excited state in ^{208}Pb. A detailed analysis of resonance parameters was carried out up to a neutron energy of 700 keV. The nuclear level density shows a strong parity dependence. The doorway in the s-wave neutron strength function has been firmly established with an escape width equal to the corresponding widths in the neighboring isotopes. The total magnetic dipole strength detected between the neutron separation energy and 8.0 MeV is $B(M1)\uparrow = 5.8\ \mu_N^2$, thus smaller than the lowest theoretical estimate for that region. Above that energy an additional 1 μ_N^2 is observed, but more strength may have escaped detection because the sensitivity of the experiment decreases; thus the "missing" strength may be partly hidden at these higher energies. Radiative widths for the $E1$ decay of resonances to the first-excited state of ^{208}Pb show a doorway structure which can be related to the properties of known bound states.

I. INTRODUCTION

The Pb isotopes are of particular interest for nuclear structure studies of unbound states. Due to the double shell closure at ^{208}Pb, the shell structure is sufficiently simple and the level density low such that model calculations can be expected to successfully predict the basic properties of states above the neutron separation energy. Indeed, simple structures have been found in s-wave neutron interaction with the Pb isotopes[1-5] and have been interpreted in terms of doorway states.[6,7]

Of particular interest are magnetic dipole transitions from 1^+ p-wave resonances to the ground state of ^{208}Pb. The question of the $M1$ strength in ^{208}Pb has been a focal point of theoretical as well as experimental work for many years. In a simple shell model, two 1^+ states are expected, resulting from 1p-1h spin-flip excitations $\nu\{(i_{13/2})^{-1}(i_{11/2})\}$ and $\pi\{(h_{11/2})^{-1}(h_{9/2})\}$ with unperturbed energies of 5.86 and 5.55 MeV, respectively. These two states mix strongly due to the residual spin- and isospin-dependent forces, yielding an "isoscalar" state at about 5.4 MeV with a reduced transition probability of $B(M1)\uparrow \approx 1$, and an "isovector" state at about 7.5 MeV which in Tamm-Daneoff approximation (TDA) has a $B(M1)\uparrow$ value of about 50 μ_N^2 (see, e.g., Vergados).[8] The latter strength may be strongly reduced by different effects like core polarization, mixing with 2p-2h configurations and Δ-hole excitations, and can be as small as 12—20 μ_N^2.[9,10] Moreover, the couplings of particles and holes to vibrations might push much of the strength to higher energies.[11]

The experimental situation has been subject to drastic changes.[12] Initially, measurements seemed to indicate a total $B(M1)\uparrow$ of 67 μ_N^2. However, subsequent reexamination by photoneutron polarization work at Argonne National Laboratory[13] (ANL) and by neutron resonance work at Oak Ridge National Laboratory[14,15] (ORNL) showed that most of the originally claimed 1^+ states were actually 1^- in character, i.e., the transitions in question were electric rather than magnetic dipole. The $M1$ strength left in the unbound region was no more than about 8 μ_N^2 for the definitely assigned 1^+ states between neutron threshold and 7.8 MeV excitation,[16] plus another tentative 8.5 MeV from possible candidates between 8.2 and 9.4 MeV identified in the photoneutron polarization data at ANL.[17]

The present work was performed in order to extend high resolution neutron resonance measurements on ^{207}Pb + n to higher energies, at the same time improving the energy resolution in the region already covered by the ORNL data. Measurements of the partial radiative capture cross sections feeding the ground state and first excited state in ^{208}Pb should help verify spin-parity assignments and more accurately determine partial radiative widths. With these measurements it was hoped to obtain additional information on the structure of unbound states in ^{208}Pb, and possibly identify additional 1^+ states and measure their ground state magnetic dipole strengths.

II. EXPERIMENTAL DETAILS

The measurements were performed at the neutron time-of-flight spectrometer of the 150 MeV electron linear accelerator of the Central Bureau for Nuclear Measurements (CBNM), Geel. A mercury-cooled uranium target served as the pulsed neutron source. The resolution of the time-of-flight spectrometer has recently been improved by the installation of a postacceleration pulse compression magnet.[18] Burst widths of 700 ps have been experimentally verified. The resulting resolution with a 400 m flight path is 100 and 700 eV at 1 and 5 MeV, respectively.

A. Total cross section measurements

Two series of transmission measurements have been performed. In the first run, covering the neutron energy range from 200 keV to 20 MeV, the detector was at a distance of 390 m from the neutron source. These measurements were carried out with an unmoderated neutron beam, i.e., detecting the neutrons from the uranium target directly. A 2 cm thick uranium filter provided a significant reduction of the γ-flash effect in the detector. For the second run, between 20 and 400 keV neutron energy, the detector was at a distance of 198 m from the source, and neutrons from two Be-canned water moderators placed directly above and below the uranium target were used. Apart from the uranium filter a B_4C filter was also used to eliminate overlap due to low energy neutrons.

The neutron detector was a 15 cm$\times$15 cm$\times$2 cm NE110 plastic scintillator with four small photomultipliers (RCA 4516), mounted sideways on the scintillator, out of the neutron beam. The construction of the detector was such as to keep capture of the incident neutrons by the construction materials very low. The pulse-height range was divided into three windows, and only those time-of-flight events for which the pulse height was within the required window were accepted. In this way, the background to signal ratio could be minimized to less than 1% over most of the energy range investigated.

The sample, placed in an automatic sample changer at a distance of 100 m from the neutron source, consisted of 255 g of enriched ^{207}Pb (92.4%) shaped in form of a disk with a thickness of 0.0363 atoms/b.

The total measuring time for both runs was about 490 h. The Linac was operated with a repetition frequency of 800 Hz and a pulse width of 700 ps. The installation of a γ-flash monitor allowed stability control of the achieved burst width. In order to deduce the background due to γ rays, a separate run was performed with a polyethylene neutron absorber in the flight path. The time dependence of the registered background was fitted with an exponential function and could later be subtracted from the measured spectra.

B. Capture γ-ray measurements

A neutron flight path of 130 m was used for the capture γ-ray measurements. Direct neutrons from the U target as well as neutrons from the water moderators were used in these measurements, which covered the neutron energy range from 1 keV to 4 MeV. Lead and B_4C filters were inserted in the neutron beam to reduce the effect of the γ flash and to prevent overlap of low-energy neutrons. An ionization chamber containing a thin uranium sample was placed 30 m from the neutron source to monitor the neutron flux shape by detecting fission fragments from the ^{235}U(n,f) reaction.

Four 7.5 cm diam and 7.5 cm thick bismuth germante (BGO) detectors were used in these measurements, mounted as shown in Fig. 1 at angles of 39°, 90°, and 125° (and 141°) with respect to the neutron beam direction (corresponding to zeros of the Legendre polynomials P_3, P_1, and P_2, respectively). The sample was reshaped to a rectangular plate of thickness 8.75×10^{-3} atoms/b.

The time-of-flight information, together with the γ-ray energy and neutron monitor spectra, were collected in list mode on a Nuclear Data 6600 data aquisition computer. The overall timing resolution of the system was approximately 4 ns. Processing of the data was done off line as described below.

In order to determine absolute capture yields, a separate measurement was performed with a 2 mm thick iron sample inserted directly in front of the lead sample, the 1.15 keV resonance[19] in ^{56}Fe serving for normalization of the products of neutron flux multiplied by detector efficiencies.

C. Elastic scattering measurements

Because for several spin 1 resonances the parities could not be determined from the transmission and radiative capture data alone, an additional elastic scattering measurement was performed. Using again a 390 m flight path, three neutron detectors were placed at different angles (39°, 90°, and 141°) with respect to the incoming beam. The detectors were NE110 plastic scintillators of 5 cm diameter and 5 cm thickness, coupled to RCA 8850 photomultipliers. In addition, two BGO detectors placed out of the scattering plane were used to record γ rays after inelastic scattering from low-lying levels in ^{207}Pb. Flux measurements were not made because only the angular distribution and the resonance shapes are important for the desired J assignments of resonances. Again, data collection was done in list mode.

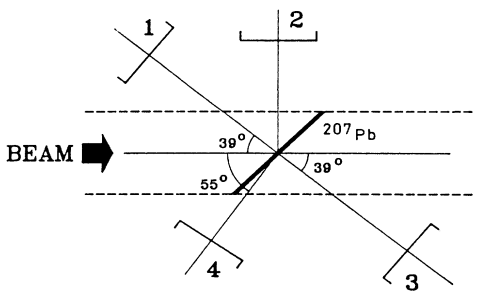

FIG. 1. Experimental layout of the neutron capture γ-ray measurements.

III. RESONANCE ANALYSIS

The resonance analysis serves to determine neutron and partial radiative widths as well as spins and parities of the resonances observed in the data. Because this is crucial for the identification of $M1$ strength, the arguments used for J^π assignments will be given special emphasis in the discussion of the data analysis.

A. Analysis of the total cross section data

After correction of the time-of-flight spectra for instrumental dead time and for backgrounds, the neutron energy corresponding to each time-of-flight channel, the total cross section, and its statistical error were calculated from the measured spectra. These data were then analyzed with the multichannel multilevel R-matrix code MULTI,[20] which was modified to allow different potential scattering radii for the various angular momentum channels.

The fitting procedure was done in two steps. We first represented the total cross section over a wide energy range (200—800 keV) by a limited number of data points characteristic of the gross structure of the cross section, i.e., omitting most of the narrow resonances. The parameters of the broad resonances (most of the s waves plus the broadest p and d waves) responsible for this gross structure were then fitted simultaneously. During this process, it turned out that in addition to the clearly visible two 1^- resonances at about 450 keV neutron energy, two broad 0^- s-wave resonances around 470 keV were necessary to fit the data. Figure 2 shows two fits to the measured cross section with and without the two 0^- resonances. The existence of these two resonances had been proposed earlier[3] on the basis of low resolution measurement and the 0^- strength is suggested on theoretical grounds,[7] but higher resolution measurements[4] had subsequently questioned the existence of these resonances. The potential scattering radii which produced the best overall fit were $R(l=0)=9.1$ fm and $R(l\neq 0)=6.4$ fm, reflecting different contributions from distant levels.

Having obtained a good representation of the gross structure, in a second step the large number of narrow resonances was analyzed separately in several narrower energy regions. For many resonances the spin and neutron orbital angular momentum could immediately be read from the peak value and the interference pattern of the total cross section. In other cases, the additional information from the capture γ-ray and elastic scattering measurements helped to assign spins and parities, as discussed below. However, a special problem arose with the parity assignment of resonances with spin $J=1$, which is crucial for the identification of $M1$ strength: Resonances with $J^\pi=1^-$ can be populated by s-wave as well as d-wave neutron interaction, and large d-wave contributions have been reported earlier.[4] In a large energy range, a certain mixing ratio of s- and d-wave contributions will result in a shape of the resonance in the total cross section very similar to the one of a $J^\pi=1^+$ p-wave resonance. Thus resonances which appear p-wave-like cannot be definitely assigned as such. Also, the γ-ray angular distribution is inconclusive in most cases, because almost every observed angular distribution can be equally well interpreted either by a 1^- assignment with s-d wave interference or by a 1^+ assignment with an appropriate channel spin mixture. Only in a few cases could negative parity be excluded by the fact that the amount of d-wave admixture necessary to explain the observed angular distribution could not be confirmed in the shape analysis of the total cross section data. These difficulties were the main reason for performing the additional elastic scattering measurements.

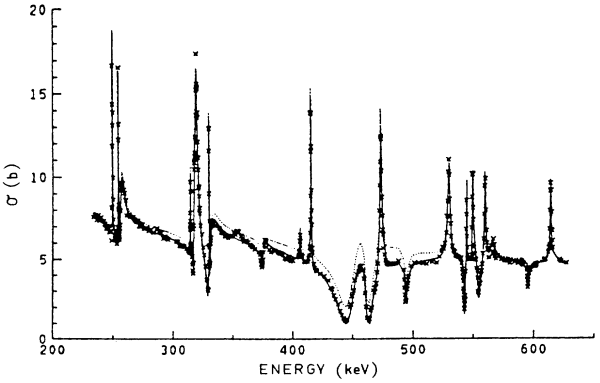

FIG. 2. R-matrix fits to the gross structure of the total cross section with (solid line) and without (dotted line) the two broad 0^- resonances.

Above the threshold for inelastic scattering at 570 keV neutron energy, an additional complication arises from the unknown inelastic width of the resonances. Due to the extra contribution to the total width, the peak cross section even of broad resonances with no resolution effect is no longer directly linked to the resonances spin. In a few cases the observation of inelastic γ rays helps to measure the inelastic width and thereby to determine the resonance spin. This is discussed in more detail below.

The resonance parameter analysis of the total cross section data has been carried through up to 700 keV neutron energy. Above that energy the resonance structure becomes too complex for a further analysis due to an increased density of observed resonances and growing uncertainty with respect to the inelastic widths.

B. Analysis of the capture γ-ray data

The off-line reduction of the capture γ-ray data was done in two steps: First, for every partial run, amplitude windows in the γ-ray spectra were fixed for the ground state transition and for the transition feeding the first excited state (3^-, 2.61 MeV) in the residual nucleus ^{208}Pb. An additional window was set at energies above the ground state transition in ^{208}Pb. It serves to obtain an estimate of the background due to scattered neutrons which interact in the BGO detectors mainly through the ^{73}Ge(n,γ) reaction. Second, the data were read back again to produce time-of-flight spectra for each of these γ-energy windows. A sample of such data, transformed to a linear energy scale, is shown together with the corresponding total cross section in Fig. 3.

Using the flux monitor data and the normalization pro-

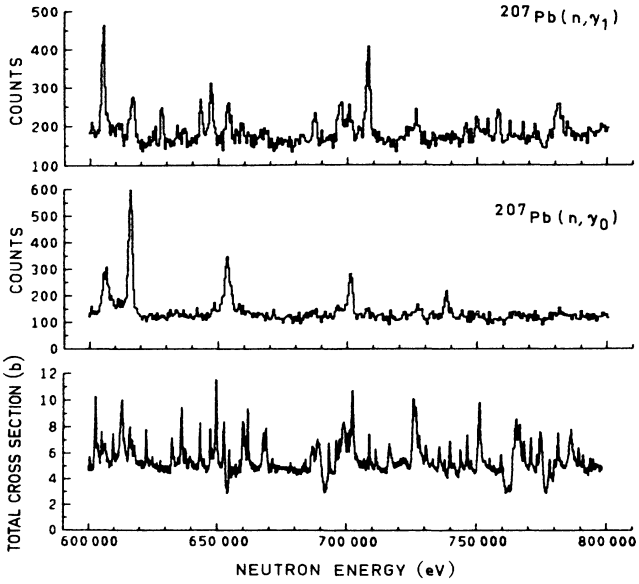

FIG. 3. Example of capture γ-ray data (top two curves) together with total cross section (lower curve).

vided by the ^{56}Fe, 1.15 keV resonance, capture yields were determined for each resonance within each of the designated pulse-height windows. Care was taken to correct the yield in each window for the scattered neutron background and the Compton contribution from higher energy γ rays. The yield data were then analyzed with a modified version of the area analysis code TACASI.[21] The code determines the partial radiative widths of a resonance, taking into account self-shielding and self-indication and performing a multiple scattering correction by means of a Monte Carlo subroutine.

The capture γ-ray data are also important in the assignment of resonance spins:

(i) Spin 0 resonances will remain unobserved in the present γ-ray data for both energy windows.

(ii) Resonances which show only a ground state transition are most probably spin 1, but the parity cannot be determined, in general, from the γ-ray data: $J^\pi=1^-$ resonances could decay weakly by an $E2$ transition to the 3^- first excited state, but in view of the reduced (by 2.61 MeV) transition energy as compared to the $E1$ ground state transition this $E2$ transition will usually not be observed. As mentioned above, the γ-ray angular distribution is also inconclusive in most cases.

(iii) Resonances which show only a transition to the 3^- first excited state will be $J \geq 2$. If transitions are observed to both the ground state and the first excited state, the radiating resonance will be $J^\pi=2^+$.

C. Analysis of the elastic scattering data

The elastic scattering data are analyzed only in a qualitative way, i.e., only the angular dependence of the resonance shapes is investigated for spin and parity assignments. To this end, theoretical cross sections for different spin-parity combinations and for the three experimental scattering angles are calculated with the Blatt-Biedenharn formalism. The calculated shapes and relative intensities are then compared to the experimental ones. Because for most resonances below about 600 keV neutron energy the spin had already been determined from the transmission and radiative capture data, the parity could be assigned or verified in this way for the majority of these resonances.

D. Inelastic γ rays

In the neutron energy region between the inelastic threshold and 700 keV, five resonances are detected in the yield of inelastic γ rays. Four of these can be identified with resonances known from the total cross section data; the fifth corresponds to a triplet of resonances which is not resolved in the inelastic γ spectra.

One of these resonances has definitely been assigned $J^\pi=2^-$ from the total and elastic scattering data. The fit of that resonance in the total cross section requires an inelastic width of 120 eV. This figure can then be used to calibrate the inelastic γ-ray yields, and with this calibration the inelastic widths of the other resonances in the inelastic γ spectrum can be determined.

IV. RESULTS AND DISCUSSION

A. Resonance parameters

For the following discussion the parameters of resonances in ^{207}Pb + n are listed in Table I. Column 1 of the table gives the resonance neutron energy. An entry in parentheses indicates that the resonance in question has not been seen in the present measurements, but has been observed additionally in total capture measurements performed with a large liquid scintillator tank at a 150 m flight path of the ORNL Linac,[22] and has been included in the table for the sake of completeness. Column 2 gives the neutron widths $g\Gamma_n$ as obtained from the analysis of the total cross section data. In columns 3 and 4 the quantities $g\Gamma_n\Gamma_\gamma/\Gamma(0^+)$ for the ground state transitions and their uncertainties, in percent, are given. Columns 5 and 6 list the corresponding quantities for the transitions to the first excited state. The errors of columns 4 and 6 include both counting statistics and an 8% normalization uncertainty common to all resonances. As long as the total width is given by the neutron width Γ_n, these quantities are equal to $g\Gamma_\gamma(0^+)$ and $g\Gamma_\gamma(3^-)$, and in the following we shall assume that this is true for all resonances of interest in the present study. Column 7 gives information on spin and parity of the resonances.

B. Level density

For a discussion of the level density, we limit ourselves to resonances with spin 0 and 1, because the density of levels with $J=2$ is very uncertain due to the large number of resonances with the assignment $J \geq 2$. We also limit ourselves to $E_n < 500$ keV, because between that energy and the inelastic threshold at 570 keV there are already five $J=1$ resonances with unknown parity. In order to arrive at an estimate for the average level spacing, we use for its spin dependence the expression (for each parity)

TABLE I. Parameters of ^{207}Pb + n resonances. Resonances with resonance energy in parenthesis are from ORNL (Ref. 22). The remaining resonances were common to the Geel and Oak Ridge measurements. The $J^{\Pi}=0, \geq 2$ assignment reflects the observation made at ORNL that the γ decay of the corresponding resonance was mainly through cascades, thus excluding $J=1$. A, (+) because of small Γ_n; B, ^{206}Pb?; C, parity from γ-ray angular distribution; D, f wave excluded; I, inelastic width observed; S, parity assignment from elastic scattering measurement.

Neutron energy (eV)	$g\Gamma_n$ (eV)	$g\Gamma_n\Gamma_\gamma/\Gamma$ ($\rightarrow 0^+$) (meV)	Error (%)	$g\Gamma_n\Gamma_\gamma/\Gamma$ ($\rightarrow 3^-$) (meV)	Error (%)	J^{Π}	Remarks
3065		6	9	35	8	2^+	
10 191		37	9	64	9	2^+	
(12 357)						$0, \geq 2$	
16 171		38	10	133	9	2^+	
16 439		13	20	13	20	2^+	
16 758	19	63	10	46	11	2^+	
29 403	20	40	16	144	11	2^+	
30 493		209	10			$1^{(+)}$	A
32 985				12	24	≥ 2	
37 747	34	508	10			1^+	
41 334	942	3233	10			1^-	
48 412		18	21	33	15	2^+	
62 836		13	25	79	12	2^+	
(67 791)						$0, \geq 2$	
68 391				56	15	≥ 2	
73 066	26	42	21			1^+	
(73 760)						$0, \geq 2$	
(75 319)							
(78 201)						$0, \geq 2$	
(79 480)						$0, \geq 2$	
82 156	19					0^+	
83 042	21	29	30	158	11	2^+	
(84 218)						$0, \geq 2$	
87 819	10	23	32			2^+	
90 242	193	1054	9			1^+	
92 998				50	16	≥ 2	
98 466	105					2^+	
101 867	45	121	15			1^-	
103 620	58					0^+	
112 141	45			87	16	≥ 2	
115 230	675	1013	10			1^+	
118 270				62	18	≥ 2	
123 840				52	23	≥ 2	
125 360		81	16	33	41		B
127 775	155	272	40	151	17	2^+	
128 020	410	1038	9	19	29	1^+	
130 327	48	563	10			1^+	C
132 293	35					(1^+)	
132 800		24	36	62	17	2^+	
135 374	23					0^+	
136 603	16	24	33	153	13	2^+	
(138 800)						$0, \geq 2$	
139 799	151					2^+	
141 120				95	16	≥ 2	
145 552	64					1^+	
(148 220)						(1^+)	
149 246	20			116	16	≥ 2	
149 770				97	16	≥ 2	
153 946	13	34	43	89	18	2^+	
154 360				33	37	≥ 2	
155 882	74	236	13			1^+	
(156 760)						$0, \geq 2$	
159 063	44			53	27	$\geq 2^+$	

TABLE I. (*Continued*).

Neutron energy (eV)	$g\Gamma_n$ (eV)	$g\Gamma_n\Gamma_\gamma/\Gamma$ ($\rightarrow 0^+$) (meV)	Error (%)	$g\Gamma_n\Gamma_\gamma/\Gamma$ ($\rightarrow 3^-$) (meV)	Error (%)	J^π	Remarks
(160 640)						$0, \geq 2$	
168 410				127	18	≥ 2	
168 650	105	45	35			1^+	
(170 660)						$0, \geq 2$	
171 314	156					2^+	
(173 880)							
179 203	85	480	11			1^+	
179 310	5					0^+	
181 150	39					1^+	
181 330	75					2^+	
181 640	43	7837	8			1^-	
182 286	7			103	20	≥ 2	
186 495	19			403	11	≥ 2	
(197 070)						$0, \geq 2$	
(199 520)						(0^+)	
(200 990)						$0, \geq 2$	
(202 070)						$0, \geq 2$	
(204 050)							
207 745	60					0^+	
208 790		69	32	117	21		B
209 590	613					2^-	S
209 591		112	32			1	
210 669	68					1^+	S
211 867	88					2^-	S
(212 480)						$0, \geq 2$	
(213 870)						$0, \geq 2$	
(216 320)						$0, \geq 2$	
217 400				28	58	≥ 2	
218 538	85					1^+	S
(220 040)						(1)	
220 355	191					2^+	S
224 108	115					2^+	S
(225 420)						$0, \geq 2$	
(226 430)						$0, \geq 2$	
228 490	2600					0^-	
229 915	467					1^+	S
(230 010)						$0, \geq 2$	
(231 340)						$0, \geq 2$	
233 347	40					$\geq 2^-$	S
240 802	30			57	38	2^+	D,S
243 632	74			118	24	2^+	D,S
244 050				143	18	≥ 2	
249 607	318	147	25			2^+	S
249 980	178	122	30			1^+	S
249 990				199	18	2	
(250 400)						$0, \geq 2$	
254 560	138			98	32	2^-	S
256 720	2020	10979	9			1^-	
(260 600)						$0, \geq 2$	
262 272	78					$\geq 2^-$	S
265 562	135					1^+	S
269 600				124	27	≥ 2	
(270 110)						$0, \geq 2$	
273 630		197	15	115	28	2^+	
(275 400)						$0, \geq 2$	
(283 250)						$0, \geq 2$	
284 794	50					1^+	
285 105	113					$(2)^+$	S

TABLE I. (*Continued*).

Neutron energy (eV)	$g\Gamma_n$ (eV)	$g\Gamma_n\Gamma_\gamma/\Gamma$ ($\rightarrow 0^+$) (meV)	Error (%)	$g\Gamma_n\Gamma_\gamma/\Gamma$ ($\rightarrow 3^-$) (meV)	Error (%)	J^Π	Remarks
287 519	46					$0, \geq 2$	
(288 940)						$0, \geq 2$	
290 327	40					0^+	
(296 470)						$0, \geq 2$	
298 035	236	473	13			1^+	C,S
300 026	36					(1^+)	
301 660				96	28	≥ 2	
(303 500)						$0, \geq 2$	
306 228	27					(1^+)	
309 280				85	29	≥ 2	
310 093	75					$\geq 2^-$	S
310 343	38					(1^-)	
314 261	165					1^+	S
317 150	61					0^+	
317 190	543	5010	9			1^-	
318 900				903	14	≥ 2	
319 670	3531					2^-	
323 455	78					2^+	
(324 820)						$0, \geq 2$	
329 912	410					3^-	
330 260	2870					1^-	
(331 340)						$0, \geq 2$	
332 566	67					$\geq 2^+$	S
335 761	130	558	12			1^+	S
336 710	119					1^+	S
345 950		63	39	94	40	2^+	
346 608	65			127	27	$\geq 2^+$	S
349 934	45					$0, \geq 2$	
355 536	88					2^-	S
359 410				74	52	≥ 2	
359 928	107					$\geq 2^+$	S
(363 450)						$0, \geq 2$	
368 904	21					2^+	S
370 230	120			119	37	$\geq 2^+$	S
(371 560)						$0, \geq 2$	
372 936	8					(0^+)	
375 080	584					0^-	
376 932	9					$0, \geq 2$	
378 785	24	103	39	520	12	2^+	
379 418	29					$0, \geq 2$	
382 696	33			430	14	2^+	S
(383 580)						$0, \geq 2$	
(385 910)						(1^+)	
389 560				130	27	≥ 2	
390 920				200	23	≥ 2	
391 920		63	48	98	31	2^+	
(392 630)						$0, \geq 2$	
395 790	229			211	23	2^+	S
396 415	18					$0, \geq 2$	
(397 800)						$0, \geq 2$	
401 691	275					2^+	S
402 644	300					2^+	S
406 010	210					0^+	
(409 800)						$0, \geq 2$	
(411 200)						$0, \geq 2$	
412 182	75					$\geq 2^+$	
413 800		314	15	345	16	2^+	
415 035	1225					3^-	

TABLE I. (*Continued*).

Neutron energy (eV)	$g\Gamma_n$ (eV)	$g\Gamma_n\Gamma_\gamma/\Gamma$ ($\rightarrow 0^+$) (meV)	Error (%)	$g\Gamma_n\Gamma_\gamma/\Gamma$ ($\rightarrow 3^-$) (meV)	Error (%)	J^Π	Remarks
(417 500)						$0, \geq 2$	
(419 900)						$0, \geq 2$	
420 806	138					1^+	S
424 450	187	225	20			1^+	S
427 367	105	171	28			1^+	S
428 624	468					2^-	S
430 420	162	67	50			1^+	S
436 581	144					0^+	
(437 600)							
(444 600)						$0, \geq 2$	
(445 600)						$0, \geq 2$	
446 477	150					2^+	S
446 500	11775					1^-	
(450 300)						$0, \geq 2$	
452 545	10			634	13	2^+	
457 622	25			173	24	≥ 2	
(460 100)						$0, \geq 2$	
461 700				184	25	≥ 2	
462 861	232					2^-	
463 880	6150					1^-	
466 528	269					1^+	S
470 000	12500					0^-	
471 682	45			190	26	$\geq 2^-$	
472 700	3325					3^-	
474 719	10						
475 571	51			379	18	$\geq 2^-$	S
478 500	5000					0^-	
479 150	25			500	14	$\geq 2^+$	S
481 419	29					$0, \geq 2$	
484 990	31						
486 495	133	297	19			1^+	S
489 040	31			1156	11	≥ 2	
489 980	75			345	16	≥ 2	
490 800	125			174	27	$2^{(+)}$	
(491 700)						$0, \geq 2$	
494 150	98			280	20	2^+	S
494 320	2549					1^-	
495 700		165	32			1	
496 974	525					3^-	
(497 600)						$0, \geq 2$	
498 857	38						
499 440	30					$(1)^+$	S
503 040				237	22	≥ 2	
504 900		189	27			1	
(506 600)						$0, \geq 2$	
(508 300)						$0, \geq 2$	
509 363	66					≥ 2	
512 073	131					1^+	S
513 253				257	23	≥ 2	
516 586	40					≥ 2	
518 050				519	15	≥ 2	
520 104	168			728	15	$\geq 2^+$	S
522 300	188			868	14	$\geq 2^+$	S
524 640				488	16	$\geq 2^-$	S
(525 900)						$0, \geq 2$	
526 830				1389	11	≥ 2	
529 000	3125					2^-	S
531 637	22						

TABLE I. (*Continued*).

Neutron energy (eV)	$g\Gamma_n$ (eV)	$g\Gamma_n\Gamma_\gamma/\Gamma$ ($\rightarrow 0^+$) (meV)	Error (%)	$g\Gamma_n\Gamma_\gamma/\Gamma$ ($\rightarrow 3^-$) (meV)	Error (%)	J^Π	Remarks
537 070				737	14	≥ 2	
538 000	75	150	34			1^+	S
538 835	87					$\geq 1^-$	
539 800				279	26	2^+	
(540 400)						1	
542 700	1087	2976	10			1^-	
543 800	625					2^+	S
548 400	38	324	17			1	
548 800	875					2^-	S
549 360		300	18	590	14	2^+	
554 390	3068	1940	13			1^-	
(554 700)						$0, \geq 2$	
555 717	68			729	14	2^-	S
555 718		370	17			1	
557 610				418	17	≥ 2	
559 190	1889					2	
559 536	38						
562 400		145	33			1	
563 800	225					1^+	S
565 270	100					0^+	
566 130	75					≥ 1	
566 890				1163	11	≥ 2	
569 007	75					≥ 1	
		Inelastic threshold					
(569 700)						$0, \geq 2$	
573 451	82			649	15	≥ 2	
(576 400)						$0, \geq 2$	
(578 300)						$0, \geq 2$	
581 629	121	181	33			1^+	S
583 431	25			385	20	≥ 2	
585 772	25					$0, \geq 2$	
587 820				276	22	≥ 2	
587 825	51						
591 200	150						
591 900	150					$0, \geq 2$	
593 300	25						
594 860	1113					1^-	
597 904	525					3	
(600 700)						$0, \geq 2$	
602 743	788					3^-	
603 800	75					0^+	
605 200	188			1937	10	$\geq 2^+$	
605 900		1005	11			1	
606 487	713	777	11			1^-	
609 732	215					1^+	S
613 100	1649					2^-	S
(613 900)						(1^+)	
616 130	450	5292	9			1^-	S
617 110	25			988	15	$\geq 2^+$	
618 034	25					$(2)^+$	
622 620	250					2^-	S,I
(624 800)						$0, \geq 2$	
628 350				745	15	≥ 2	
(631 700)						$0, \geq 2$	
632 745	375					$\geq 1^+$	S
636 421	625					≥ 2	
637 849	75						

TABLE I. (*Continued*).

Neutron energy (eV)	$g\Gamma_n$ (eV)	$g\Gamma_n\Gamma_\gamma/\Gamma$ ($\rightarrow 0^+$) (meV)	Error (%)	$g\Gamma_n\Gamma_\gamma/\Gamma$ ($\rightarrow 3^-$) (meV)	Error (%)	J^π	Remarks
(640 400)						$0, \geq 2$	
643 500	375			896	14	≥ 2	
645 087	75						
(646 000)						$0, \geq 2$	
647 467	75			1483	11	≥ 2	
648 480		360	21			1	
649 655	1050					3	
652 538	731						
653 692	113					1	I
(653 700)						$0, \geq 2$	
653 870	1389	4180	9			1^-	
654 680	164					$0, \geq 2$	
659 805	60						
660 217	700						I
661 013	25						
661 832	700						I
(663 600)						$0, \geq 2$	
667 420	200						
667 700	150						
667 980	150						
668 880	250					4^+	I
670 000	75						
671 399	38						
(672 800)						$0, \geq 2$	
(674 500)						$0, \geq 2$	
684 359	38						
686 500	75						
686 976	188					1	I
687 400				585	17	2^+	
688 810	860						
689 640	75						
691 800	975					1^-	
693 388	500						B
696 200	452	315	21			1^+	I
697 528	250			1000	14	≥ 2	
698 709	100						
699 108	750						
699 588	100						
			Only selected resonances				
701 500		1974	11			$1^{(-)}$	
702 450						3	
708 100		288	28	2079	10	2^+	
(722 400)						$0, \geq 2$	
726 620		523	18	688	16	2^+	
727 800		299	28			1	
(734 400)						$0, \geq 2$	
738 500		880	14			1^-	S
(741 600)						$0, \geq 2$	
745 600				276	31	≥ 2	
750 000				536	21	≥ 2	
(751 700)						$0, \geq 2$	
754 100				271	35	≥ 2	
758 100				751	15	≥ 2	
(773 300)						$0, \geq 2$	
781 400				1196	15	2^-	
(786 000)							B
(794 000)						$0, \geq 2$	

TABLE I. (*Continued*).

Neutron energy (eV)	$g\Gamma_n$ (eV)	$g\Gamma_n\Gamma_\gamma/\Gamma$ ($\rightarrow 0^+$) (meV)	Error (%)	$g\Gamma_n\Gamma_\gamma/\Gamma$ ($\rightarrow 3^-$) (meV)	Error (%)	J^Π	Remarks
799 000		320	32	445	26	2^+	S
(804 600)						2^+	
(809 700)						$0, \geq 2$	
(813 300)						$0, \geq 2$	
818 400				587	21	≥ 2	
820 600		745	17			1^-	S
(823 700)						$0, \geq 2$	
(827 700)						$0, \geq 2$	
829 500				562	23	≥ 2	
(835 200)						$0, \geq 2$	
(839 100)						$0, \geq 2$	
842 490		793	18			1^-	S
(843 100)						$0, \geq 2$	
(847 000)						$0, \geq 2$	
847 300		1100	13			1	
849 700		1126	13			1	
851 770				306	32	≥ 2	
857 000		1488	14			1^-	S
859 080				315	32	≥ 2	
911 200		1529	13			1^-	S
953 300		647	19			1	
956 500		1349	14			1	
974 600				412	34	≥ 2	
995 000		1009	20			$1^{(+)}$	S
1 000 800		1210	16			1	
1 005 000				584	34	≥ 2	
1 111 600		733	23			1	
1 167 200		1773	15			1	
1 218 300		599	28			1	
1 230 000		730	24			1	
1 287 000		1524	18			1	
1 320 000		941	30			1	
1 330 000		2287	17			1	

$$D(J^\pi)=D_0/(2J+1)\exp[-J(J+1)/2\sigma^2] ,$$

with a spin cutoff parameter $\sigma=4.55$ from Gilbert and Cameron,[23] and adopt in the range 0–500 keV all resonances with $J=0$ and 1, including those resonances for which the spin assignment is uncertain (in parentheses in Table I), thus, totally, 15 spin 0 resonances and 47 spin 1 resonances. This yields for the parameter D_0 an average value of

$$D_0=62\pm 6 \text{ keV} .$$

The D_0 values obtained for spin 0 and spin 1 resonances separately are 66 ± 9 and 61 ± 6 keV, respectively, thus in perfect agreement with the assumed spin dependence.

However, this average results from rather different level densities for the two parities. For a determination of the parity dependence, we use only those resonances below 500 keV neutron energy with a definite spin-parity assignment. We obtain

$$D(\pi=-1)/D(\pi=+1)=2.8\pm 0.4 .$$

For each parity separately, this yields

$$D_0(\pi=-1)=118\pm 18 \text{ keV}$$

and

$$D_0(\pi=+1)=42\pm 5 \text{ keV} .$$

The indicated errors include both an estimated 10% uncertainty due to possible missed resonances and resonances with uncertain spin-parity assignments and the statistical uncertainty due to the orthogonal ensemble distribution for a limited sample.

C. Neutron strength distribution

1. s-wave resonances

The cumulative sums of reduced neutron widths $g\Gamma_n$ of *s*-wave resonances is shown in Fig. 4, together with the corresponding sums for the two neighboring isotopes.[1,5]

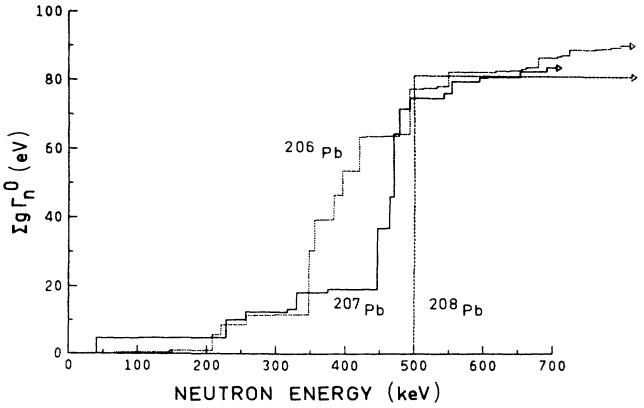

FIG. 4. Cumulative sums of reduced neutron widths of ^{207}Pb + n s-wave resonances as compared to the corresponding resonances in ^{208}Pb + n (Ref. 1) and ^{206}Pb + n (Ref. 5).

The figure demonstrates the importance of the two broad $J^\pi=0^-$ resonances at 470.0 and 478.5 keV neutron energy (mentioned already in Sec. III A) in addition to the broad $J^\pi=1^-$ resonances at 446.5, 463.9, and 494.3 keV. The presence of these two 0^- resonances assures the existence of a doorway state in both the $J^\pi=0^-$ and 1^- s-wave channels, and only by including them is the $g(J)$-weighted sum of the escape widths the same for all three isotopes, as required in the weak coupling picture of Divadeenam *et al.*[7]

2. *p-wave resonances*

Figure 5 shows, on an arbitrary scale, the cumulative sum of reduced neutron widths $g\Gamma_n^1$ for $J^\pi=1^+$ resonances. Again, a doorway state is apparent around 120 keV neutron energy. The figure also includes the cumulative sum of reduced magnetic dipole transition strengths for decay to the ^{208}Pb ground state. It is obvious that the two curves have a similar shape, indicating that we are dealing with a doorway common to both channels.[24] For the resonances below 200 keV neutron energy, the correlation coefficient between the two reduced strengths is

$$c=0.80\ .$$

This correlation suggests a fairly simple picture for the configurations involved, such as the incoming neutron dropping into the $p_{1/2}$ hole in ^{207}Pb and exciting the expected $M1$ $\nu\{(i_{13/2})^{-1}(i_{11/2})\}$ and $\pi\{(h_{11/2})^{-1}(h_{9/2})\}$ spin flip transitions. However, a strong doorway-like p-wave resonance is also present at about the same neutron energy in ^{206}Pb + n,[5] and in ^{208}Pb + n,[25] suggesting a particle-vibration origin. Moreover, the cumulative $B(M1)\uparrow$ strength of the states up to 200 keV is only about 4.3 μ_N^2, i.e., much less than any theoretical estimate. As discussed below, we have to assume that the $M1$ spin flip strength is much more fragmented, and that the apparent common doorway at about 120 keV is at least partly of different origin.

We conclude this subsection by listing, in Table II, p-wave neutron strength functions as obtained from the cumulative sums of reduced neutron widths of resonances up to 700 keV neutron energy. These strength functions, with the possible exception of the $J^\pi=2^+$ strength function, will not be very sensitive to missed resonances or resonances not definitely assigned with respect to J^π values because such problems will generally concern small resonances. A channel radius of $a_c=8.0$ fm has been used. The resulting p-wave strength function, although much smaller than the optical model calculation[26] in this mass region, agrees well with measured values for neighboring isotopes (see Ref. 26).

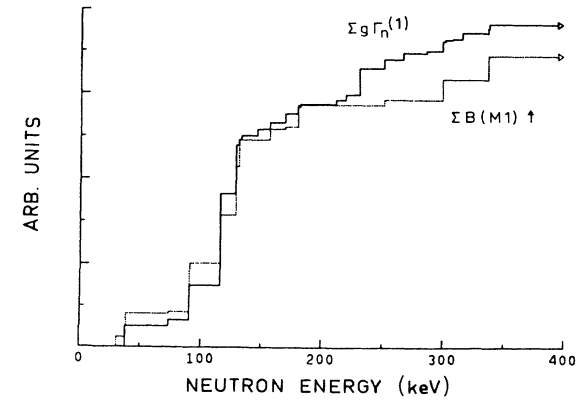

FIG. 5. Comparison of the cumulative sums of reduced neutron widths and reduced magnetic dipole strengths for ground state transitions of $J^\Pi=1^+$ resonances. The vertical scales are chosen to show clearly the presence of a common doorway state.

D. Magnetic dipole strength

The results obtained with respect to the expected magnetic dipole strength are illustrated in Fig. 6. In the upper half of this figure the distribution of the reduced magnetic dipole strength as determined from the ground state decays of those resonances definitely assigned as $J^\pi=1^+$ is plotted. The sum of these strengths is $\sum B(M1)\uparrow=6.8$ μ_N^2. In the lower half all resonances assigned $J=1$ are shown, including those with undetermined parity but excluding known 1^- resonances. The resonances without parity assignments are mainly those at higher energies ($E_n>700$ keV), which have been detected in the capture

TABLE II. p-wave strength functions. (The indicated errors are mainly due to the statistical uncertainty of the Porter-Thomas distribution for a limited sample.)

J^Π	$S(l,J)$ (10^{-4})	error	
0^+	0.20	$+0.11$ -0.06	$S(l=1)=0.27^{+0.05}_{-0.04}\times10^{-4}$
1^+	0.63	$+0.16$ -0.12	
2^+	0.23	$+0.06$ -0.04	

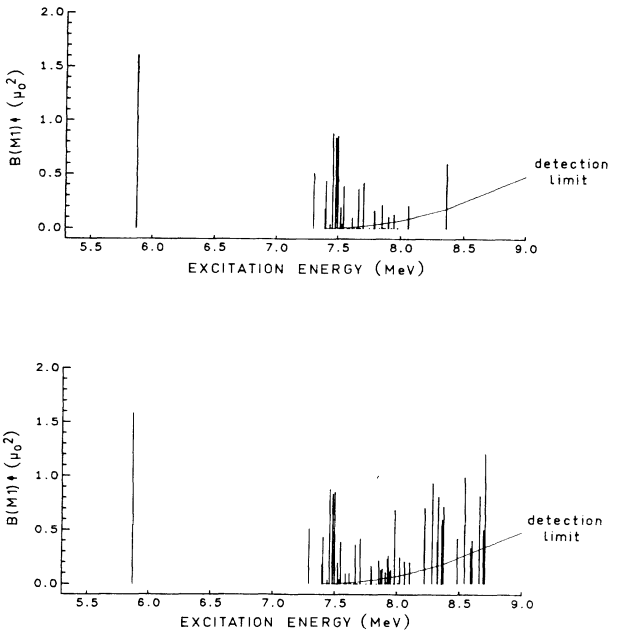

FIG. 6. Distribution of reduced magnetic dipole strength in ^{208}Pb. Upper half: measured strength of definitely assigned 1^+ states. Lower half: including also those $J=1$ resonances with unknown parity identified in the present work. The strong bound state at 5.8 MeV is from Wienhard *et al.* (Ref. 27).

measurements due to their relatively strong ground state transition but which cannot be clearly identified in the transmission data and consequently cannot be given a parity assignment. Including all these resonances, the sum of reduced strengths increases to 17.7 μ_N^2.

However, most, if not all, of the γ-ray strength observed in the $J=1$ resonances with undetermined parity will be $E1$ rather than $M1$ radiation. This can be seen from the following argument. Below 500 keV neutron energy, most $J=1$ resonances have been detected and their parities assigned. Thus $E1$ and $M1$ "strength functions" (cumulative sums of strengths per energy interval) can be estimated. In the $M1$ case the strength function is taken in the energy range between 300 and 500 keV in order to exclude the doorway state around 120 keV. With these, the "expected" $E1$ and $M1$ strengths between 500 and 1300 keV can be estimated and it turns out that the missing $E1$ strength alone is larger than what corresponds to the observed transitions from the $J=1$ resonances with undetermined parity. This leads to the conclusion that the majority of the strong transitions shown at the higher energies in the lower part of Fig. 6 are, in fact, not of $M1$ character.

On the other hand, the increasing detection limit shown in Fig. 6 indicates that most of the $J^\pi=1^+$ resonances at the higher energies will have escaped detection unless they happened to be very strong. Also, at neutron energies above about 800 keV ($E_{ex}>8.2$ MeV), the widths for inelastic neutron emission may start to contribute significantly to the total width; this would reduce the measured quantities $g\Gamma_n\Gamma_\gamma/\Gamma$ and eventually preclude detection and measurement of radiative strengths at still higher energies. If the "background strength function" determined between 300 and 500 keV neutron energy is assumed constant towards higher energies, the expected $M1$ strength between 500 and 1300 keV would be 3.9 μ_N^2 as compared to the 1.1 μ_N^2 actually assigned in that range. This estimate would bring the total $M1$ strength between the neutron separation energy at 8.7 MeV excitation to 9.6 μ_N^2

The only statement which can finally be made with respect to the 500—1300 keV region (7.9—8.7 MeV excitation energy) is that there is no reason to take the observed strong transitions from resonances with $J=1$ but unassigned parity as an indication of another doorway-like concentration of $M1$ strength in this region. Some of the numerical values mentioned in this discussion are summarized in Table III.

Apart from these strengths above the neutron separation energy, there is an additional 1.6 μ_N^2 due to the bound state at 5.846 MeV found by Wienhard *et al.*,[27] and 0.5 μ_N^2 at 7.279 MeV found by Moreh *et al.*[28] The 5.846 MeV state is most probably the theoretically predicted[8] isoscalar 1^+ state in ^{208}Pb.

E. Transitions to the first-excited state of ^{208}Pb.

Many resonances are observed to show relatively strong radiative transitions to the first excited state of ^{208}Pb (see Fig. 3). The majority of these transitions will be of electric dipole character. If all of them are assumed $E1$, and the cumulative sum of reduced transition strengths is plotted as a function of energy, Fig. 7 results. A doorway-type behavior is observed with a summed strength within the doorway of $B(E1)\downarrow\approx 0.15\ e^2\,\mathrm{fm}^2$.

It is interesting to note that two $J^\pi=1^-$ bound states are known to exist at about 5.4 MeV excitation energy in ^{208}Pb which are probably of 1p-1h character and decay to the ground state by strong $E1$ transitions with $\sum B(E1)\downarrow\approx 0.19\ e^2\,\mathrm{fm}^2$.[29] If we add to their excitation energy the energy of the 3^- first excited state of 2.6 MeV, we arrive at 8.0 MeV, which corresponds to the 600 keV neutron energy where the doorway is observed. It is thus tempting to assume that the doorway consists of the same particle-hole configuration weakly coupled to the 3^- vi-

TABLE III. Summed magnetic dipole strengths.

Energy range	Cumulative strength (μ_N^2)
Detected, 0—200 keV	4.3
Detected, 0—500 keV	5.7
Detected, 0—1300 keV	6.8
0—1300 keV, missed levels estimated by extrapolation	9.6
0—1300 keV, including $J=1$ resonances with unknown parity	17.7

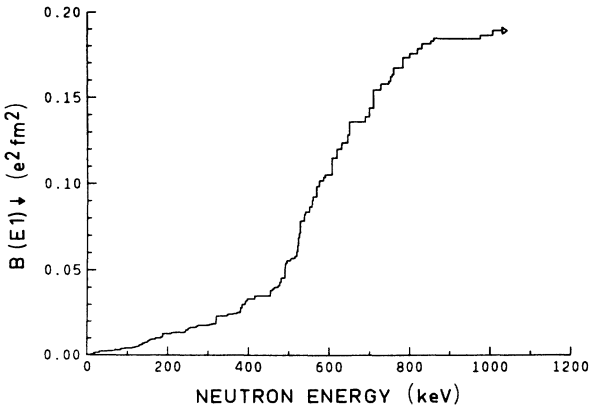

FIG. 7. Cumulative sum of reduced $E1$ transition strengths for decay of the observed resonances to the first excited state of ^{208}Pb.

bration, and that we are dealing with the same basic transition with the 3^- vibrational state acting merely as a spectator.

V. CONCLUSION

High resolution measurements of neutron interaction with ^{207}Pb have improved our knowledge of this interesting system. The debated doorway in the $J^\pi=0^-$ s-wave channel has been firmly established, and the summed escape widths of the doorway states in both s-wave channels equal the corresponding widths in the neighboring isotopes ^{208}Pb and ^{206}Pb, as predicted in a weak coupling model.

Partial radiative widths for transitions to the ground state and the first excited state of ^{208}Pb have been determined for many resonances with firmly assigned spin and parity. The known doorway state in the $J^\pi=1^+$ p-wave neutron channel is seen to act as a common doorway also for the $M1$ ground state radiative transitions, but its cumulative strength is only 4.3 μ_N^2. The total magnetic dipole strength detected above the neutron separation energy is $\sum B(M1)\uparrow=6.8\ \mu_N^2$, compared to the lowest theoretical estimate[10] of 12.4 μ_N^2. However, the appreciable fragmentation of $M1$ strength observed suggests that considerable strength is missed in the upper part of the energy range investigated (excitation energies above 8 MeV). Unfortunately, the decreasing sensitivity of the present experiment precludes a reliable estimate of the amount of strength at these higher energies.

An interesting new feature is observed in the radiative decay of resonances to the first-excited state of ^{208}Pb. The radiative widths show a doorway structure which, if assumed to be due to $E1$ radiation, has a total strength equal to the known strength of two 1^- bound states. This suggests that the 3^- vibrational state acts as a mere spectator in a weak coupling situation.

ACKNOWLEDGMENTS

We wish to thank J. van Audenhove and J. M. Salomé, responsible for the preparation of the ^{207}Pb samples and the linac operation, respectively. This work was supported in part by the U.S. Department of Energy under Contract No. DE-AC05-84-OR21400 with Martin Marietta Energy Systems, Inc.

[1]J. L. Fowler and E. C. Campbell, Phys. Rev. **127**, 2192 (1962).
[2]J. A. Farrell, G. C. Kyker, Jr., E. G. Bilpuch and H. W. Newson, Phys. Lett. **17**, 286 (1965).
[3]F. T. Seibel, E. G. Bilpuch, and H. W. Newson, Ann. Phys. (N.Y.) **69**, 451 (1972).
[4]D. J. Horen, J. A. Harvey, and N. W. Hill, Phys. Rev. C **18**, 722 (1978).
[5]D. J. Horen, J. A. Harvey, and N. W. Hill, Phys. Rev. C **20**, 478 (1979); **24**, 1961 (1981).
[6]M. Divadeenam and W. P. Beres, in *Proceedings of the International Conference on Statistical Properties of Nuclei*, Albany, 1971, edited by J. B. Garg (Plenum, New York, 1972), p. 579.
[7]M. Divadeenam, W. P. Beres, and H. W. Newson, Ann. Phys. (N.Y.) **80**, 231 (1973).
[8]J. D. Vergados, Phys. Lett. **36B**, 12 (1971).
[9]E. Lipparini and A. Richter, Phys. Lett. **144B**, 13 (1984).
[10]D. Cha, B. Schwesinger, J. Wambach, and J. Speth, Nucl. Phys. **A430**, 321 (1984).
[11]G. E. Brown, J. S. Dehesa, and J. Speth, Nucl. Phys. **A330**, 290 (1979).
[12]G. E. Brown and S. Raman, Comments Nucl. Part. Phys. **9**, 79 (1980).
[13]R. J. Holt, R. M. Laszewski, and H. E. Jackson, Phys. Rev. C **15**, 827 (1977).
[14]D. J. Horen, J. A. Harvey, and N. W. Hill, Phys. Lett. **67B**, 268 (1977).
[15]D. J. Horen, G. F. Auchampaugh, and J. A. Harvery, Phys. Lett. **79B**, 39 (1978).
[16]S. Raman, M. Mizumoto, and R. L. Macklin, Phys. Rev. Lett. **39**, 598 (1977).
[17]R. J. Holt, H. E. Jackson, R. M. Laszewski, and J. R. Specht, Phys. Rev. C **20**, 93 (1978).
[18]D. Tronc, J. M. Salome, and K. H. Böckhoff, Nucl. Instrum. Methods **228**, 217 (1985).
[19]R. E. Chrien, M. R. Bhat, and O. A. Wasson, Phys. Rev. C **1**, 973 (1970); R. E. Chrien, private communication.
[20]G. F. Auchampaugh, Los Alamos Scientific Laboratory Scientific Report LA-5473-MS, 1974 (unpublished).
[21]F. H. Fröhner, General Atomic Report GA-6906, 1966.
[22]K. A. Griffioen, private communication.

[23]A. Gilbert and A. G. W. Cameron, Can. J. Phys. **43**, 1446 (1965).

[24]L. C. Dennis and S. Raman, in *Proceedings of the 5th International Symposium on Capture Gamma Ray Spectroscopy and Related Topics,* Knoxville, 1984, edited by S. Raman (AIP, New York, 1985), p. 495.

[25]D. J. Horen, C. H. Johnson, J. L. Fowler, A. D. MacKellar, and B. Castel, Phys. Rev. C **34**, 429 (1986).

[26]S. F. Mughabghab, M. Divadeenam, and N. E. Holden, *Neutron Cross Sections* (Academic, New York, 1981), Vol. 1.

[27]K. Wienhard, K. Ackerman, K. Bangert, U. E. P. Berg, C. Bläsing, W. Naatz, A. Ruckelshausen, D. Rück, R. K. M. Schneider, and R. Stock, Phys. Rev. Lett. **49**, 18 (1982).

[28]R. Moreh, S. Shlomo, and A. Wolf, Phys. Rev. C **2**, 1144 (1970).

[29]M. J. Martin, Nucl. Data Sheets **47**, 797 (1986).